Water Oxidation

DOI: 10.1002/ange.201402407

Ligand Modification Transforms a Catalase Mimic into a Water Oxidation Catalyst**

*Wei-Tsung Lee, Salvador B. Muñoz III, Diane A. Dickie, and Jeremy M. Smith**

Abstract: *The catalytic reactivity of the high-spin Mn^{II} pyridinophane complexes $[(Py_2NR_2)Mn(H_2O)_2]^{2+}$ (R = H, Me, tBu) toward O_2 formation is reported. With small macrocycle N-substituents (R = H, Me), the complexes catalytically disproportionate H_2O_2 in aqueous solution; with a bulky substituent (R = tBu), this catalytic reaction is shut down, but the complex becomes active for aqueous electrocatalytic H_2O oxidation. Control experiments are in support of a homogeneous molecular catalyst and preliminary mechanistic studies suggest that the catalyst is mononuclear. This ligand-controlled switch in catalytic reactivity has implications for the design of new manganese-based water oxidation catalysts.*

Manganese plays an important role in biological dioxygen chemistry, particularly at the active sites of oxygen-evolving enzymes, including manganese catalase (MnCAT) and the oxygen-evolving center (OEC) of Photosystem II. In the case of MnCAT, O_2 is formed from the catalytic disproportionation of hydrogen peroxide. The active site of MnCAT has two Mn ions bridged by carboxylate and single-atom ligands, likely water and/or hydroxide.[1,2] As implied by its name, the OEC, which contains a Mn_4Ca cluster held together by bridging carboxylates and oxo ligands, is the site at which photosystem II oxidizes water to O_2.[3] Although there is little sequence homology between MnCAT and the OEC, it is striking that the best structural matches to the OEC almost all come from binuclear manganese enzymes, including MnCAT. This observation has fuelled the hypothesis that the inorganic core of the OEC may have derived from manganese catalase.[4] It is thus tempting to speculate on the relationship between the catalytic reactivities of MnCAT and the OEC.

The water oxidation reactivity of the OEC has attracted substantial attention in the development of catalysts for solar-driven water oxidation, particularly those that are based on inexpensive and earth-abundant first-row transition metals.[5] The mechanism by which the OEC produces O_2 is still far from resolved. Reaction pathways involving both single and multiple Mn ions of the cluster have been proposed,[6] making the rational design of bioinspired manganese complexes for water oxidation difficult. Thus, in contrast to the plethora of manganese complexes that are functional models for MnCAT,[7] water oxidation by synthetic solution-phase Mn catalysts is still relatively undeveloped.[8–10] A limited number of "single-turnover" manganese complexes have been shown to stoichiometrically evolve O_2 from water or hydroxide.[11] Catalytic O_2 production in the presence of water has been demonstrated for some mono- and multinuclear Mn complexes;[12–15] however, these studies generally use chemical oxidants having indeterminate chemical innocence.[16] Electrochemically driven O_2 formation in the presence of multinuclear Mn complexes has been reported, typically in non-aqueous solvents;[14,17,18] however, little is known about the stability of these complexes under catalytic conditions, where decomposition to catalytically active heterogeneous materials is a possibility.

We have previously shown that the pyridinophane complex $[Mn(Py_2NMe_2)(H_2O)_2]^{2+}$ (**2**; Figure 1) is a robust catalyst for hydrogen peroxide disproportionation. The pyridinophane macrocycle provides the same donor functionality as some open-chain aminopyridine ligands that facilitate the electrochemical oxidation of Mn^{II}–OH_2 complexes to $[Mn^{IV}(\mu\text{-}O)_2Mn^{IV}]$ dimers under basic conditions.[19] Mechanistic investigations show that the oxidation is coupled to a proton transfer from the aqua ligands,[20] which is reminiscent of water oxidation catalysts that form M=O intermediates by coupled electron/proton transfer events.[21] Inspired by these results as well as the potential relationship between catalase and water oxidation reactivity, we hypothesized that pyridinophane ligands may provide the appropriate combination of properties required for manganese water oxidation cata-

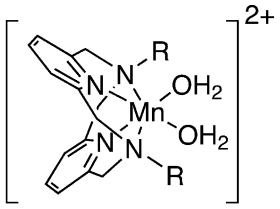

R = H (**1**), Me (**2**), *t*Bu (**3**)

Figure 1. Structure of $[Py_2NR_2Mn(H_2O)_2]^{2+}$ complexes.

[*] Dr. W.-T. Lee, S. B. Muñoz III, Prof. J. M. Smith
Department of Chemistry, Indiana University
800 East Kirkwood Ave., Bloomington, IN 47405 (USA)
E-mail: smith962@indiana.edu
Dr. D. A. Dickie
Department of Chemistry and Chemical Biology
The University of New Mexico
Albuquerque, NM 87131 (USA)

[**] Funding from Indiana University, the American Chemical Society (Petroleum Research Foundation, 50971-ND3), and the U.S. Department of Energy (Office of Basic Energy Sciences; DE-FG02-08ER15996) is gratefully acknowledged. J.M.S. is a Dreyfus Teacher-Scholar. S.B.M. acknowledges support from NIH-RISE (R25 GM06122211). We thank Song Xu, Dennis Chen, and Sara Skrabalak for experimental assistance.

Supporting information for this article is available on the WWW under http://dx.doi.org/10.1002/anie.201402407.

lysts.[22] Thus, in addition to having a donor character that is similar to that of the aminopyridine ligands mentioned above, these ligands also have tunable steric properties that are expected to obviate dimer formation and possibly lead to O_2 formation.

In this contribution, we investigate the effect of pyridinophane ligand modifications on the catalytic properties of $[Mn(Py_2NR_2)(H_2O)_2]^{2+}$ complexes, showing that changes to the amine donor switches catalysis from hydrogen peroxide disproportionation to water oxidation. Importantly, both types of catalysis occur in aqueous solution. This observation has implications for the design of new manganese water oxidation catalysts.

Reaction of Py_2NR_2 (R = H, *t*Bu) with $MnBr_2$ yields the high-spin Mn^{II} complexes $(Py_2NR_2)MnBr_2$,[23] similar to other Mn pyridinophanes.[24,25] In neutral aqueous solution the manganese ions are solvated as $[(Py_2NR_2)Mn(H_2O)_2]^{2+}$ **1** and **3** (Figure 1), as determined by conductivity and mass spectrometry measurements.

As mentioned above, we had previously shown that **2** is a robust catalyst for hydrogen peroxide disproportionation. Similarly to this earlier work, we find that hydrogen peroxide is catalytically disproportionated by **1** (Figure 2), which

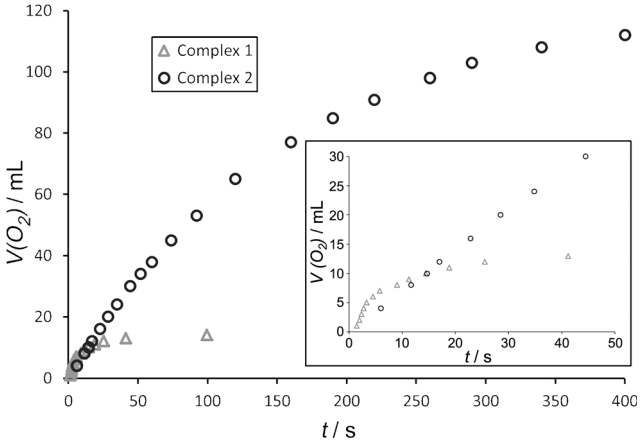

Figure 2. Dioxygen formation from catalytic hydrogen peroxide disproportionation catalyzed by complexes **1** and **2**. Initial conditions: [Mn] = 0.4 mM, $[H_2O_2]$ = 3.7 M, pH 3.9, 298 K. Inset: Formation of O_2 over the first 50 seconds of catalysis.

contains a less bulky pyridinophane ligand. Catalysis is observed over a wide pH range (pH 3.9–9) in aqueous solution. The rate of hydrogen peroxide disproportionation for **1** (initial rate = 86(9) μmol s^{-1} at pH 3.9) is faster than for the previously reported complex **2** (initial rate = 27(5) μmol s^{-1}). However, in comparison with **2**, the longevity of complex **1** is attenuated. Thus, lower turnover numbers (TONs) are observed for **1** (TON 830 at pH 3.9) than for **2** (TON up to 58000).[25] In contrast to **1** and **2**, complex **3**, which has the bulkiest pyridinophane ligand, shows no evidence for hydrogen peroxide disproportionation. Thus, pyridinophane ligand modification switches off disproportionation catalysis, perhaps due to the increased bulk of the amine substituents.

The three complexes also show different electrochemical behavior in aqueous solution. The cyclic voltammograms of **3** in basic aqueous solution display large irreversible waves that are pH-dependent (Figure 3). For example, with a glassy

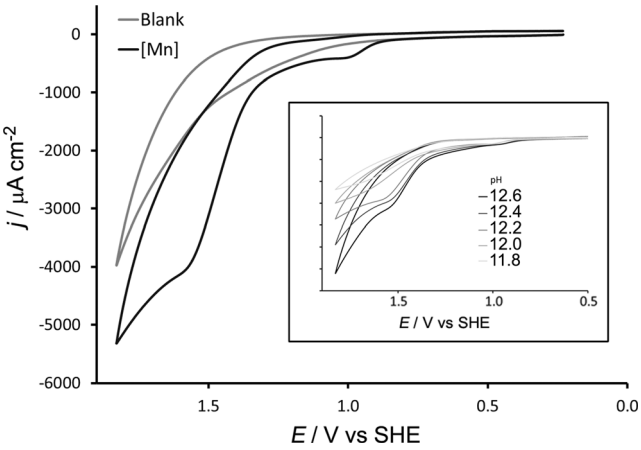

Figure 3. Cyclic voltammograms of solutions with and without **3** (0.5 mM) at pH 12.2 in aqueous solution. Experimental conditions: 50 mM KOTf, 100 mV s^{-1} scan rate, GC electrode. Inset: Cyclic voltammograms of **3** as a function of pH.

carbon (GC) disk electrode (0.07 cm^2), the cyclic voltammogram between 0 to 1.8 V (vs. SHE) at pH 12.2 shows a wave at ca. 1.0 V, followed by a large irreversible wave with an onset potential of approximately 1.3 V. Similar results are obtained under the same conditions with a fluorine-doped tin oxide (FTO) working electrode.[26] Importantly, solutions of Mn^{2+} do not display similar behavior under the same conditions. In contrast to **3**, there is no evidence for electrocatalysis in the cyclic voltammograms of complexes **1** and **2** in basic solution.[26]

Additional experiments have been undertaken to characterize the electrocatalytic behavior of **3**. The formation of bubbles on the FTO electrode is observed over several scans, concomitant with the appearance of a broad wave at around −0.3 V versus SHE. This wave disappears when the cell is purged with N_2, leading us to assign it to the O_2/O_2^- couple.[27] Complex **3** is therefore a catalyst for the electrochemical oxidation of water to O_2. The onset potential for electrocatalysis at pH 12.2 (ca. 1.3 V) corresponds to an overpotential for water oxidation of about 0.8 V, which is in the range reported for many homogeneous water oxidation catalysts.[28]

The catalytic performance of **3** has been evaluated in an N_2-purged, gas-tight cell. Controlled-potential electrolysis at +1.23 V versus SHE (foot of the wave)[29] shows that the charge passed is greater in the presence of **3** than for the pure electrolyte solution or in the presence of Mn^{2+} (Figure 4). The formation of O_2 during electrolysis has been characterized by a number of methods. A Clark-type electrode shows a steady increase in dissolved O_2 during bulk electrolysis. Gas-phase O_2 has been characterized by thermal conductivity gas chromatography following the bulk electrolysis experiment. As expected for water oxidation, the pH of the unbuffered solution decreases over the course of the electrolysis experi-

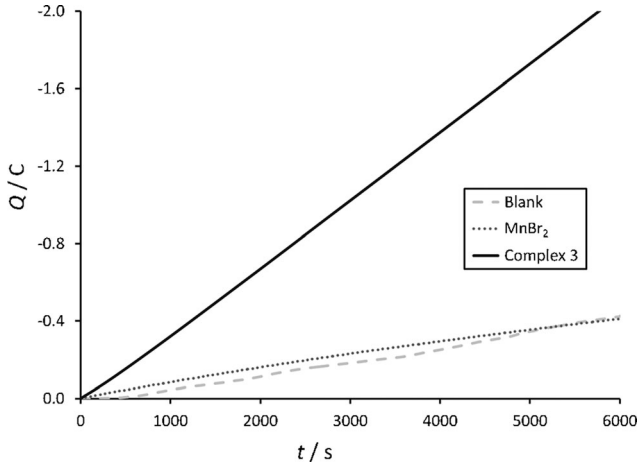

Figure 4. Charge passed during controlled-potential electrolysis without manganese (light gray dashed line), with 25 μM $MnBr_2$ (gray dots), and with 25 μM **3** (black solid line). Initial pH 12.2, 2.5 mM KOTf, FTO electrode. Electrolysis potential = 1.23 V versus SHE (foot of the wave).[29]

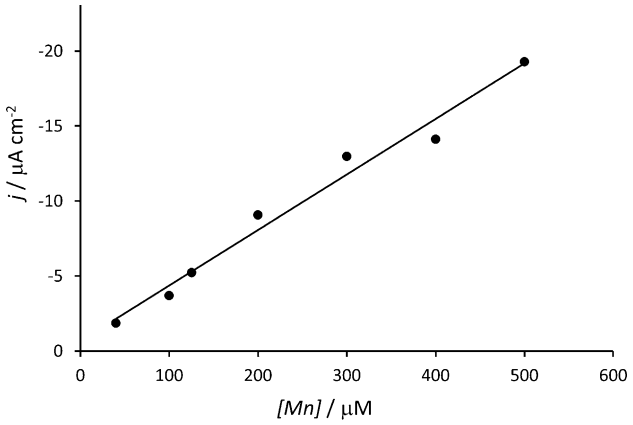

Figure 5. Plot of the catalytic current as a function of the catalyst concentration for complex **3**. The background current has been subtracted.

ment. A number of electrolysis experiments gave turnover numbers of 16–24 with Faradaic efficiencies of 74–81%.

Other working electrode materials did not give better results. With reticulated vitreous carbon, a substantial degradation of the electrode is observed, whereas the formation of brown deposits on the electrode surface occurs when an indium-doped tin oxide (ITO) electrode is used.

A number of experiments have been undertaken to exclude the possibility of heterogeneous or nanoparticle catalysts; this situation has been shown to occur with other nominally homogenous water oxidation electrocatalysts.[30] No new bands are observed in the optical spectrum of the electrolysis solution, suggesting that the formation of nanoparticles is unlikely. This observation is corroborated by dynamic light scattering measurements of these solutions that provide no evidence for nanoparticles.[31] There is also no evidence for the formation of a heterogeneous electrocatalytic deposit on the electrode surface. The catalytic current does not increase over successive cyclic voltammetric (CV) scans, which would be expected for the formation of a catalytic deposit. In addition, there are no significant changes in the optical spectrum of the FTO electrode following electrolysis. Finally, there is no evidence by energy-dispersive X-ray (EDX) measurements for the formation of Mn-containing deposits on the electrode. Thus, all evidence available points to a homogeneous molecular catalyst for water oxidation.

Initial mechanistic experiments indicate that the catalytic current varies linearly with the concentration of **3**, consistent with a mononuclear catalyst for water oxidation (Figure 5). Based on the precedent of other single-site electrocatalysts[32] and the first-order dependence of the rate on catalyst concentration, we suggest that water oxidation involves the formation of a high-valent manganese oxo intermediate that is attacked by H_2O/OH^- to form the O–O bond.

Both steric and electronic factors appear to play a role in facilitating water oxidation by **3**. For example, whereas **1** can be oxidized to form a dimer containing a $[Mn(\mu\text{-}O)_2Mn]$ core,[26] the analogous transformation is not observed for **3**. This is likely a consequence of the bulky Py_2NtBu_2 macrocycle substituents that prevent dimer formation. Additionally, in the cyclic voltammogram the first oxidation wave is observed at a lower potential for **3** ($E_a \approx 1.0$ V) than the corresponding waves for **1** and **2** ($E_a \approx 1.2$ V). Thus, access to higher oxidation states is more facile for **3**, likely due to the greater donor strength of the Py_2NtBu_2 macrocycle.

The foregoing results show how a simple ligand modification converts an aqueous-phase hydrogen peroxide disproportionation catalyst into a water oxidation catalyst. Ongoing mechanistic work is aimed at elucidating the water oxidation pathway as well as the origin of the pyridinophane substituent effect on catalytic reactivity. It is nonetheless intriguing at this stage to consider that existing mononuclear manganese complexes for hydrogen peroxide disproportionation may also be endowed with water oxidation capabilities by simple ligand modification.

Experimental Section

General experimental details and characterization data are included in the Supporting Information. CCDC-983498, 983499, and 999618 contain the supplementary crystallographic data for this paper. These data can be obtained free of charge from The Cambridge Crystallographic Data Centre via www.ccdc.cam.ac.uk/data_request/cif.

Received: February 13, 2014
Revised: June 17, 2014
Published online: July 15, 2014

Keywords: catalysis · macrocycles · manganese · molecular electrochemistry · water splitting

[1] A. J. Wu, J. E. Penner-Hahn, V. L. Pecoraro, *Chem. Rev.* **2004**, *104*, 903–938.

[2] a) S. V. Antonyuk, V. R. Melik-Adamyan, A. N. Popov, V. S. Lamzin, P. D. Hempstead, P. M. Harrison, P. J. Artymyuk, V. V. Barynin, *Crystallogr. Rep.* **2000**, *45*, 105–116; b) V. V. Barynin, M. M. Whittaker, S. V. Antonyuk, V. S. Lamzin, P. M. Harrison, P. J. Artymiuk, J. W. Whittaker, *Structure* **2001**, *9*, 725–738.

[3] a) J. P. McEvoy, G. W. Brudvig, *Chem. Rev.* **2006**, *106*, 4455 – 4483; b) H. Dau, I. Zaharieva, M. Haumann, *Curr. Opin. Chem. Biol.* **2012**, *16*, 3 – 10.

[4] a) A. Williamson, B. Conlan, W. Hillier, T. Wydrzynski, *Photosynth. Res.* **2011**, *107*, 71 – 86; b) J. Raymond, R. E. Blankenship, *Coord. Chem. Rev.* **2008**, *252*, 377 – 383.

[5] P. Du, R. Eisenberg, *Energy Environ. Sci.* **2012**, *5*, 6012 – 6021.

[6] a) P. E. M. Siegbahn, *Acc. Chem. Res.* **2009**, *42*, 1871 – 1880; b) S. Yamanaka, H. Isobe, K. Kanda, T. Saito, Y. Umena, K. Kawakami, J.-R. Shen, N. Kamiya, M. Okumura, H. Nakamura, K. Yamaguchi, *Chem. Phys. Lett.* **2011**, *511*, 138 – 145.

[7] S. Signorella, C. Hureau, *Coord. Chem. Rev.* **2012**, *256*, 1229 – 1245.

[8] X. Liu, F. Wang, *Coord. Chem. Rev.* **2012**, *256*, 1115 – 1136.

[9] For a critical evaluation of water oxidation catalysis by homogenous Mn complexes, see V. Artero, M. Fontecave, *Chem. Soc. Rev.* **2013**, *42*, 2338 – 2356.

[10] See the Supporting Information (Tables S1–S3) for a summary of previous reports of water oxidation by homogeneous manganese complexes as well as a comparison with other electrocatalysts based on 3d transition metals (Table S4).

[11] a) Y. Shimazaki, T. Nagano, H. Takesue, B.-H. Ye, F. Tani, Y. Naruta, *Angew. Chem.* **2004**, *116*, 100 – 102; *Angew. Chem. Int. Ed.* **2004**, *43*, 98 – 100; b) Y. Gao, T. Åkermark, J. Liu, L. Sun, B. Åkermark, *J. Am. Chem. Soc.* **2009**, *131*, 8726 – 8727.

[12] Recent reviews: a) C. W. Cady, R. H. Crabtree, G. W. Brudvig, *Coord. Chem. Rev.* **2008**, *252*, 444 – 455; b) M. Wiechen, H.-M. Berends, P. Kurz, *Dalton Trans.* **2012**, *41*, 21 – 31.

[13] Photochemical water oxidation by a multinuclear Mn complex: E. A. Karlsson, B.-L. Lee, T. Åkermark, E. V. Johnston, M. D. Kärkäs, J. Sun, Ö. Hansson, J.-E. Bäckvall, B. Åkermark, *Angew. Chem.* **2011**, *123*, 11919 – 11922; *Angew. Chem. Int. Ed.* **2011**, *50*, 11715 – 11718.

[14] Electrocatalytic water oxidation in the presence of a multinuclear Mn complex in aqueous solution: Y. Gao, R. H. Crabtree, G. W. Brudvig, *Inorg. Chem.* **2012**, *51*, 4043 – 4050.

[15] a) R. K. Seidler-Egdal, A. Nielsen, A. D. Bond, M. J. Bjerrumb, C. J. McKenzie, *Dalton Trans.* **2011**, *40*, 3849 – 3858; b) K. J. Young, M. K. Takase, G. W. Brudvig, *Inorg. Chem.* **2013**, *52*, 7615 – 7622.

[16] a) H. Chen, R. Tagore, G. Olack, J. S. Vrettos, T.-C. Weng, J. Penner-Hahn, R. H. Crabtree, G. W. Brudvig, *Inorg. Chem.* **2007**, *46*, 34 – 43; b) M. Yoshida, S. Masaoka, J. Abe, K. Sakai, *Chem. Asian J.* **2010**, *5*, 2369 – 2378; c) D. J. Wasylenko, C. Ganesamoorthy, M. A. Henderson, B. D. Koivisto, H. C. Osthoff, C. P. Berlinguette, *J. Am. Chem. Soc.* **2010**, *132*, 16094 – 16106; d) D. J. Wasylenko, C. Ganesamoorthy, M. A. Henderson, C. P. Berlinguette, *Inorg. Chem.* **2011**, *50*, 3662 – 3672; e) A. R. Parent, R. H. Crabtree, G. W. Brudvig, *Chem. Soc. Rev.* **2013**, *42*, 2247 – 2252; f) D. G. H. Hetterscheid, J. N. Reek, *Eur. J. Inorg. Chem.* **2014**, 742 – 749.

[17] Y. Naruta, M. Sasayama, T. Sasaki, *Angew. Chem.* **1994**, *106*, 1964 – 1965; *Angew. Chem. Int. Ed. Engl.* **1994**, *33*, 1839 – 1841.

[18] Substoichiometric amounts of O_2 (maximum TON = 0.05) were observed in the constant potential electrolysis of mononuclear Mn complexes in nonaqueous solvent, see T. Gao, J. H. Liu, M. Wang, Y. Na, B. Åkermark, L. Sun, *Tetrahedron* **2007**, *63*, 1987 – 1994.

[19] See for example, a) C. Hureau, G. Blondin, M.-F. Charlot, C. Philouze, M. Nierlich, M. Césario, E. Anxolabéhère-Mallart, *Inorg. Chem.* **2005**, *44*, 3669 – 3683; b) S. Groni, C. Hureau, R. Guillot, G. Blondin, G. Blain, E. Anxolabéhère-Mallart, *Inorg. Chem.* **2008**, *47*, 11783 – 11797.

[20] B. Lassalle-Kaiser, C. Hureau, D. A. Pantazis, Y. Pushkar, R. Guillot, V. K. Yachandra, J. Yano, F. Neese, E. Anxolabéhère-Mallart, *Energy Environ. Sci.* **2010**, *3*, 924 – 938.

[21] C. J. Gagliardi, A. K. Vannucci, J. J. Concepcion, Z. Chen, T. J. Meyer, *Energy Environ. Sci.* **2012**, *5*, 7704 – 7717.

[22] a) C. M. Che, Z. Y. Li, K. Y. Wong, C. K. Poon, T. C. W. Mak, S. M. Peng, *Polyhedron* **1994**, *13*, 771 – 776; b) S. P. Meneghetti, P. J. Lutz, J. Fischer, J. Kress, *Polyhedron* **2001**, *20*, 2705 – 2710; c) M. Graf, G. Wolmershäuser, H. Kelm, S. Demeschko, F. Meyer, H.-J. Krüger, *Angew. Chem.* **2010**, *122*, 962 – 965; *Angew. Chem. Int. Ed.* **2010**, *49*, 950 – 953; d) J. R. Khusnutdinova, J. Luo, N. P. Rath, L. M. Mirica, *Inorg. Chem.* **2013**, *52*, 3920 – 3932.

[23] The complexes have also been crystallographically characterized as the acetonitrile solvate.

[24] B. Albela, C. Carina, S. Policar, S. Poussereau, J. Cano, J. Guilheim, L. Tchertanov, G. Blondin, M. Delroisse, J.-J. Girerd, *Inorg. Chem.* **2005**, *44*, 6959 – 6966.

[25] W.-T. Lee, S. Xu, D. A. Dickie, J. M. Smith, *Eur. J. Inorg. Chem.* **2013**, 3867 – 3873.

[26] See the Supporting Information for more details.

[27] K. Ichinose, Y. Kimikado, T. Yoshida, *Electrochemistry* **2011**, *79*, 146 – 155.

[28] See for example, a) J. J. Concepcion, J. H. Jurss, M. K. Brennaman, P. G. Hoertz, A. O. T. Patrocinio, N. Y. M. Iha, J. L. Templeton, T. J. Meyer, *Acc. Chem. Res.* **2009**, *42*, 1954 – 1965; b) S. M. Barnett, K. I. Goldberg, J. M. Mayer, *Nat. Chem.* **2012**, *4*, 498 – 502; c) M.-T. Zhang, Z. Chen, P. Kang, T. J. Meyer, *J. Am. Chem. Soc.* **2013**, *135*, 2048 – 2051.

[29] C. Costentin, S. Drouet, M. Robert, J.-M. Savéant, *J. Am. Chem. Soc.* **2012**, *134*, 11235 – 11242.

[30] a) N. D. Schley, J. D. Blakemore, N. K. Subbaiyan, C. D. Incarvito, F. D'Souza, R. H. Crabtree, G. W. Brudvig, *J. Am. Chem. Soc.* **2011**, *133*, 10473 – 10481; b) J. J. Stracke, R. G. Finke, *J. Am. Chem. Soc.* **2011**, *133*, 14872 – 14875; c) B. Limburg, E. Bouwman, S. Bonnet, *Coord. Chem. Rev.* **2012**, *256*, 1451 – 1467.

[31] The detection limit for the DLS experiment is 40 nm, whereas the sensitivity is 0.1 ppm.

[32] a) J. J. Concepcion, J. W. Jurss, J. L. Templeton, T. J. Meyer, *J. Am. Chem. Soc.* **2008**, *130*, 16462 – 16463; b) D. J. Wasylenko, C. Ganesamoorthy, J. Borau-Garcia, C. P. Berlinguette, *Chem. Commun.* **2011**, *47*, 4249 – 4251; c) D. J. Wasylenko, R. D. Palmer, C. P. Berlinguette, *Chem. Commun.* **2013**, *49*, 218 – 227.